Fabrication of Self-Supported Patterns of Aligned β-FeOOH Nanowires by a Low-Temperature Solution Reaction

Yujie Xiong,[a] Yi Xie,*[a] Shaowei Chen,[b] and Zhengquan Li[a]

Abstract: Self-supported patterns of oriented alignment of β-FeOOH nanowires are fabricated through a simple solution reaction from the complex $[Fe(phen)_3]^{2+}$ at 60 °C. The alignment of nanowires with a diameter of 40 nm and length of 6 μm is relatively uniform. HRTEM studies show that the growing direction of β-FeOOH nanowires is perpendicular to the orientation plane of self-formed β-FeOOH flake-like substrates. In the reaction and crystal growth process, the precursor $[Fe(phen)_3]^{2+}$ is undoubtedly vital to the formation of nanowire alignment. In detail, the formation of aligned nanowires is thought to be realized by controlling two competing reactions. Electrochemical and UV-visible measurements suggest that the product might have potential applications in lithium batteries and semiconductor electronics. This synthetic process is simple, mild, clean, reproducible, and free of any template; it provides a novel pathway for the low-temperature growth of nanowires and their simultaneous oriented alignment.

Keywords: alignment · FeOOH · iron · nanostructures · oriented wires

Introduction

Nanowires (which are one-dimensional (1D) objects), as the smallest dimension structures for efficient transport of electrons, can be applied to detect the theoretical operating limits of lithium batteries.[1] Recent research on nanowires is expanding rapidly into their assembly to two- (2D) and three-dimensional (3D) ordered superstructures.[2–6] In the past years, due to the anisotropic structure of nanowires, their alignments are mainly focused on the solid template method,[2] such as porous alumina and polymer nanotubes. Recently, a vapor-phase-transport patterned-catalyst growth technique[3] has been reported to fabricate oriented alignment of ZnO nanowires, pioneering a new area of chemical methods to fabricate nanowire alignment. All these methods utilized templates to control the directional growth on the heterogeneous substrates. A solution reaction route has also been developed to construct nanowire alignment on SnO_2 or Al_2O_3 substrates.[4] There have been some reports attempting to create self-supported (that is, supported on the self-formed homogeneous substrates), aligned 1D nanocrystals by simple and mild chemical reactions;[5] however, the obtained structures grow radially, not highly oriented. As for the electrode materials, fabrication methods of their nanowire alignments are limited in hard template techniques.[6] Thus seeking a simple and convenient way to fabricate oriented nanowire alignment is necessary.

The development of new positive electrode materials has been of interest up to now. Iron compounds seem to be very attractive for the production of large-scale lithium batteries, because of their large natural abundance and low cost. Recently, β-FeOOH, which exhibits a tunnel-type structure in which the iron atoms are strongly bonded to the framework that constitutes the tunnels, has been reported to be a promising candidate for an active iron-based material for lithium batteries.[7] This material has a more stable structure in which the possibility of structural collapse is eliminated, and lithium ions can be intercalated in the tunnels, resulting in its potential applications as positive electrode materials. Moreover, β-FeOOH is a semiconductor with the band gap of 2.12 eV[8] and can also be used in oxidation/reduction reactions and hydroprocessing of coal as catalysts,[9] in the pigment industry,[10] and in the preparation of ferromagnetic materials, such as γ-Fe_2O_3.[10] Thus, oriented alignment of β-FeOOH nanowires might have potential applications in lithium batteries, semiconductor electronics, and preparation of magnetic recording media materials. In this paper, we describe a simple solution reaction based on $[Fe(phen)_3]^{2+}$

[a] Prof. Y. Xie, Dr. Y. Xiong, Dr. Z. Li
Structure Research Laboratory and Department of Chemistry
University of Science and Technology of China
Hefei, Anhui 230026, (P. R. China)
Fax: (+86) 551-3603987
E-mail: yxielab@ustc.edu.cn

[b] Prof. S. Chen
Department of Chemistry
Southern Illinois University
Carbondale, Illinois 62901-4409 (USA)
E-mail: schen@chem.siu.edu

Supporting information for this article is available on the WWW under http://www.chemeurj.org or from the author.

 DOI: 10.1002/chem.200305118

(phen = 1,10-phenanthroline) to fabricate self-supported patterns of oriented alignment of β-FeOOH nanowires. To the best of our knowledge, this is the first case that a self-supported pattern of oriented alignment of nanowires is fabricated by means of a low-temperature solution route.

Results and Discussion

Phase and purity of as-obtained product—X-ray diffraction (XRD) pattern: The as-obtained product powder was determined by the X-ray diffraction (XRD) pattern, shown in Figure 1. All the reflection peaks can be indexed to pure

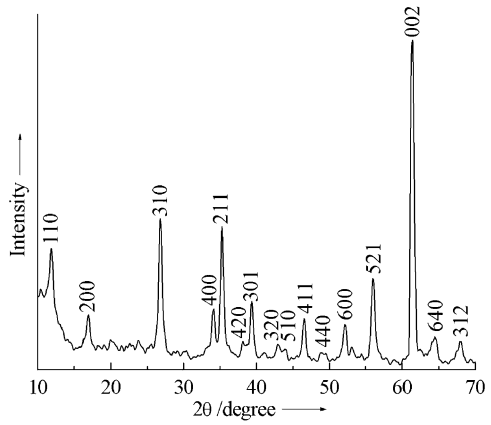

Figure 1. The XRD pattern of the oriented alignment of β-FeOOH nanowires, showing evident orientation along (002) plane.

tetragonal β-FeOOH (JCPDS card 34-1266, $a = 10.535$ Å, $c = 3.030$ Å). No characteristic peak was observed for other impurities such as α-Fe_2O_3 and γ-Fe_2O_3. The (002) peak intensity has been evidently increased in the obtained XRD pattern, implying the β-FeOOH nanowires align along the [001] axis. The peaks of other crystal planes still appear in the XRD pattern, due to the fact that this pattern was measured on the powder sample in which the nanowires were randomly mixed.

The morphology and growth direction of as-obtained product: The morphology of the product was examined by the field emission scanning electron microscopy (FE-SEM), whereby the solid sample was mounted on a copper slice without any dispersion treatment. One can observation (Figure 2A and B) that the nanowires are aligned mostly in the same direction. More direct observation of the cross section (Figure 2C(3)) reveals that the nanowires with a diameter of 40 nm and length of 6 μm are densely aligned and relatively straight. From a blank part near the fringe of aligned nanowires (Figure 2C(1)) and a naked fringe of flake (Figure 2C(2)), it is found that the aligned nanowires grow on flake-like substances that have irregular edges of several micrometers. More careful observations of these regions show that the nanowires near the fringes of flakes have less density, shorter length, and less order alignment. The energy dispersive X-ray analyses (EDXA) of both the nanowires and the supporting-

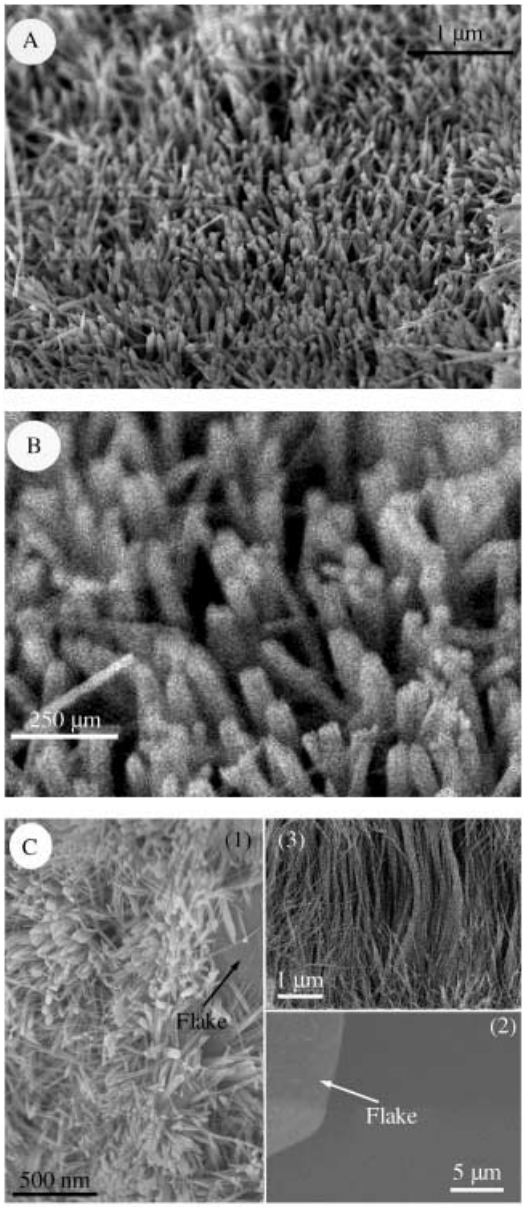

Figure 2. A) and B) FE-SEM images of the oriented alignment of β-FeOOH nanowires without any treatment. C) FE-SEM images of 1) the aligned nanowires and the blank part near the fringe; 2) the naked fringe of flakes, revealing the aligned nanowires grow on flakes; and 3) the cross section of oriented-aligned nanowires.

flakes show the Fe and O composition to be that of β-FeOOH. These results clearly show the oriented alignment of β-FeOOH nanowires supported on self-formed β-FeOOH flakes.

The product was further investigated by high-resolution transmission electron microscopy (HRTEM), whereby the sample was treated by ultrasonic dispersion in ethanol for 30 min and then put onto a copper grid. TEM observations (Figure 3A and C) show that after ultrasonic dispersion treatment, the oriented alignments are destroyed and the nanowires and the supporting-flakes were entirely separated. The one-dimensional HRTEM image of the nanowires (Figure 3B) shows that the as-obtained nanowires are structurally uniform and crystalline. The interdistance of lattice planes is

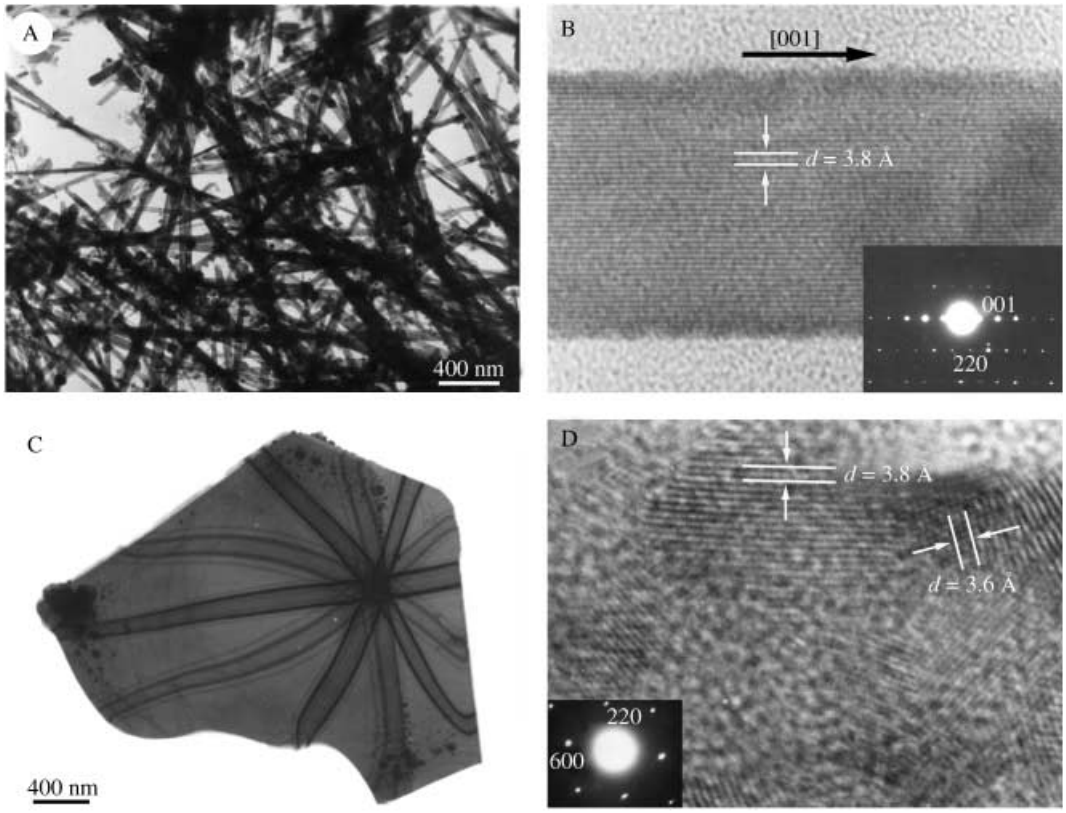

Figure 3. A) TEM image of β-FeOOH nanowires after ultrasonic dispersion treatment. B) HRTEM image and electron diffraction pattern of β-FeOOH nanowires. C) TEM image of β-FeOOH flake-like substrates after ultrasonic dispersion treatment. D) HRTEM image and electron diffraction pattern of β-FeOOH flake-like substrates.

approximately 3.8 Å, which can be indexed to the (002) plane. Meanwhile, the electron diffraction pattern (inset in Figure 3B) can be indexed to the [1 1 0] zone axis of tetragonal β-FeOOH, further confirming that the nanowires are crystalline and grow along [001] axis. Figure 3C shows a typical TEM image of flakes, in which the texture results from the electron beam on the thin layer of sample.[11] In the two-dimensional HRTEM image of the flakes (Figure 3D), lattice planes can clearly be seen ($d = 3.8$, 3.6 Å) and indexed to the (220) and (300) planes of tetragonal β-FeOOH, respectively. The electron diffraction pattern (inset in Figure 3D) of the flakes can be indexed to [001] zone axis of tetragonal β-FeOOH, revealing that the flake-like substrates are oriented along the (001) plane. All these results indicate that the growing direction of nanowires is vertical to the orientation plane of flakes. The EDXA of both the nanowires and the supporting-flakes show the Fe and O in the composition of β-FeOOH. These EDXA results performed with TEM are in good agreement with those from SEM.

Possible formation mechanism of self-supported patterns of aligned β-FeOOH nanowires: In the current work, the precursor of $[Fe(phen)_3]^{2+}$ is undoubtedly vital to the formation of nanowire alignment. In previous research, although many other routes were developed to prepare 1D β-FeOOH,[12] no oriented alignment of 1D objects has been observed. It indicates that the formation of these nanostructures does not result from the structural characteristics of β-FeOOH.

A convenient and basic route to β-FeOOH in previous research is to carry out the hydration and oxidation/hydrolysis of Fe^{2+} or hydrolysis of Fe^{3+} ions. Those reactions are too rapid, resulting in the difficulty of controlling the crystal growth of β-FeOOH. In our approach to the oriented alignment of 1D β-FeOOH, the complexing reagent of 1,10-phenanthroline slows down the oxidization/hydrolysis of Fe^{2+} ions, so that the reactions proceed more slowly to provide enough time for the growth of β-FeOOH crystal. It can also adsorb to specific surfaces to affect the morphology of the crystals.

From the structural characteristics, $[Fe(phen)_3]^{2+}$ has a distorted octahedral structure, which can be gradually hydrated to $[Fe(H_2O)_2(phen)_2]^{2+}$, $[Fe(H_2O)_4phen]^{2+}$, and $[Fe(H_2O)_6]^{2+}$ [Eqs. (1)–(4)].

$$[Fe(phen)_3]^{2+} + 2H_2O \leftrightarrow [Fe(H_2O)_2(phen)_2]^{2+} + phen \quad (1)$$

$$[Fe(H_2O)_2(phen)_2]^{2+} + 2H_2O \leftrightarrow [Fe(H_2O)_4phen]^{2+} + phen \quad (2)$$

$$[Fe(H_2O)_4phen]^{2+} + 2H_2O \leftrightarrow [Fe(H_2O)_6]^{2+} + phen \quad (3)$$

$$4[Fe(H_2O)_6]^{2+} + O_2 \rightarrow 4\beta\text{-}FeOOH + 8H^+ + 18H_2O \quad (4)$$

The resulting $[Fe(H_2O)_6]^{2+}$ can be oxidized and hydrolyzed into β-FeOOH in air,[13] which ensures the completion of the hydration from $[Fe(phen)_3]^{2+}$ to $[Fe(H_2O)_6]^{2+}$. It is noteworthy that the phen ligand can stabilize Fe^{2+}, preventing $[Fe(phen)_3]^{2+}$ from oxidization by air.[13] With the dissociation of phen and the hydration of $[Fe(phen)_3]^{2+}$, the complexes of

Fe^{2+} are more and more inclined to be oxidized by air. For example, a little $[Fe(H_2O)_2(phen)_2]^{2+}$ can be oxidized to $[Fe(H_2O)_2(phen)_2]^{3+}$, which can also eventually form β-FeOOH [Eqs. (5)–(8)].

$$4[Fe(H_2O)_2(phen)_2]^{2+} + O_2 + 2H_2O \rightarrow 4[Fe(H_2O)_2(phen)_2]^{3+} + 4OH^- \quad (5)$$

$$[Fe(H_2O)_2(phen)_2]^{3+} + 2H_2O \leftrightarrow [Fe(H_2O)_4phen]^{3+} + phen \quad (6)$$

$$[Fe(H_2O)_4phen]^{3+} + 2H_2O \leftrightarrow [Fe(H_2O)_6]^{3+} + phen \quad (7)$$

$$[Fe(H_2O)_6]^{3+} \rightarrow \beta\text{-}FeOOH + 3H^+ + 4H_2O \quad (8)$$

Thus, the first-degree hydration process will most probably form two products: $[Fe(H_2O)_2(phen)_2]^{2+}$ and $[Fe(H_2O)_2(phen)_2]^{3+}$, shown as the complex **I** and **II**, respectively, in Scheme 1. In complex **I**, the Fe^{2+} ion has a d^6 high-spin structure, and the two ligands of phen lie on an approximate square plane.[14] Hence, there exists planar steric inhibition for the later oxidization/hydrolysis reactions; this leads to the preferential oxidization/hydrolysis along its normal direction. This is advantageous for the growth of β-FeOOH nanowires along [001] axis by the oxidization and hydrolysis processes. In complex **II**, the Fe^{2+} ions with d^5 structure have larger splitting energy than Fe^{3+} ions, and the two ligands of phen tend not to from a plane;[13] thus, the steric inhibition along the normal direction of the complex results in the preferential hydrolysis at the plane and, hence, the formation of β-FeOOH flakes with (001) orientation. Evidently, the oxidization degree from complex **I** to complex **II** is relatively low and the first hydration process is more inclined to produce **I**. Thus, it should be more undemanding to produce the nanowires than the flakes, resulting in the production of a mass of nanowires and a small quantity of flakes. Since the axis growth plane of nanowires is consistent with the orientation plane of flakes, the nanowires should grow easily on the flakes in an oriented manner.

The reaction temperature is also an important parameter in the fabrication of these nanostructures. Most probably, a kinetic control is needed to form both the complexes **I** and **II** at the same time, which in turn results in the simultaneous formation of nanowires and flakes. Since the oxidization from complex **I** to **II** evidently needs a relatively high temperature, a temperature of 60 °C is required for the simultaneous formation of nanowires and flakes. Our experiments indicate that the products prepared at room temperature are all nanowires without flakes supporting. However, at too high reaction temperatures, rapid hydration and oxidization/hydrolysis reactions occur, and none of the desired nanostructures are obtained. For example, only β-FeOOH with polyhedron morphology is obtained at 100 °C.

The electrochemical properties of as-obtained product: The Mössbauer spectrum reveals that residual chlorine content of β-FeOOH is relative low; thus, the sample has more sites to accommodate lithium, resulting in its potential application for positive electrode material in lithium batteries. Figure 4 shows

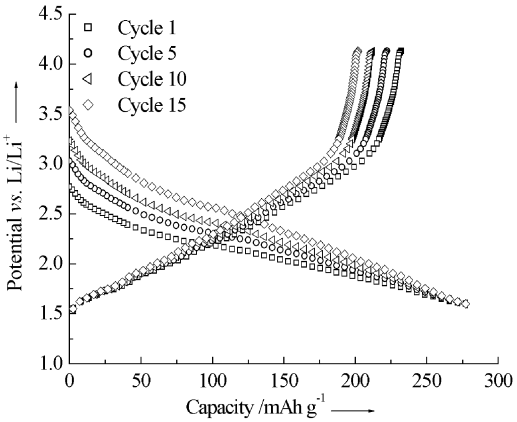

Figure 4. Charge and discharge curves of the sample.

the charge and discharge curves of the as-obtained product, which were obtained by using $LiClO_4$/(2 ethylene chloride + 2 dimethyl chloride + diethyl chloride) as electrolyte in a glass cell. The cell was first discharged to intercalate the lithium ions in the tunnels and then charged to extract them at a current density of 0.1 mA cm^{-2}. During the process of first discharge, the cell shows a plateau at around 2 V and a

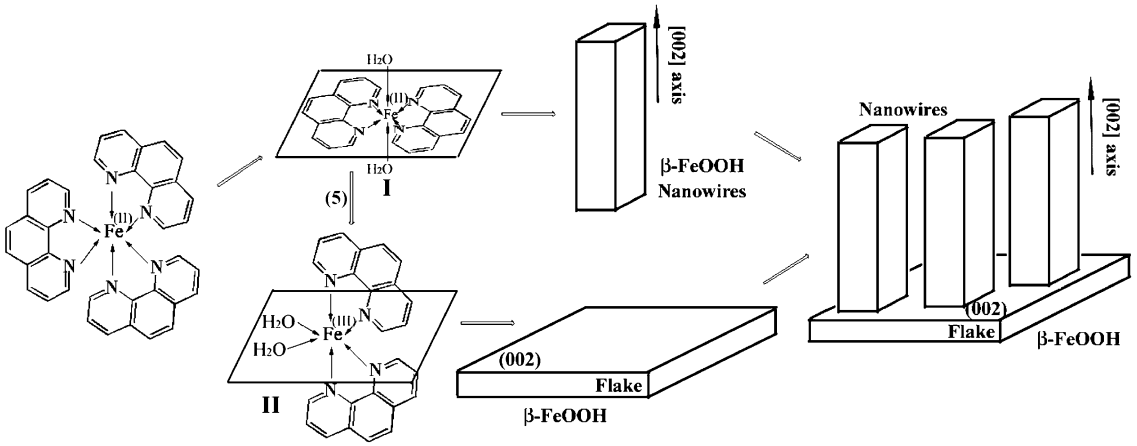

Scheme 1. Schematic formation illustration of the oriented alignment of nanowires growing on self-formed flakes.

capacity of over 278 mA h g^{-1}. These experimental data show that proton de-intercalation is very difficult, and only lithium intercalation and de-intercalation occur as the following reaction [Eq. (9)].

$$\beta\text{-FeOOH} + Li^+ + e^- \rightarrow FeOOHLi \quad (9)$$

The measured capacity of the sample is very close to the theoretical one (283 mA h g^{-1}) calculated from this reaction and the reported experimental one of bulk β-FeOOH;[7] this indicates that approximately one lithium ion could be intercalated and extracted from the tunnels. It was also confirmed by elemental analysis of discharged material, which gives a composition of $FeOOHLi_{0.95}$. During the second discharge, the potential of the cell increased slightly to 2–2.5 V. The overall discharge capacity of the sample after 15 cycles was almost the same as that of the first cycle (278 mA h g^{-1}), revealing that the charge and discharge cycles run well.

The X-ray photoelectron spectra (XPS) were used to analyze the sample before and after discharge. Figure 5A and B show the XPS core level spectrum of Fe 2p orbitals of the sample before and after discharge, respectively. The position of the Fe $2p_{3/2}$ peak of the sample before discharge (712.5 eV) is consistent with that of trivalent iron as reported in Fe_2O_3[15] and bulk β-FeOOH. The Fe 2p peaks after the discharge are shifted toward low binding energy, and the observed $2p_{3/2}$ binding energy of the discharged sample (708.1 eV) is consistent with the reported data of divalent Fe.[15] It indicates that trivalent iron is reduced to the divalent state during lithium insertion in the tunnels upon discharging. Figure 5C shows the XPS core level spectrum of Li 1s orbitals for the discharged sample. The position of the Li 1s peak (57.1 eV) is very close to that of LiCl (56.9 eV), in which lithium is purely ionic,[15] revealing that the lithium in the tunnel after discharge is purely ionic. Therefore, the good cyclic reversibility of the sample observed in the electrochemical performance measurements should be contributed to the pure ionic state of lithium in the tunnels that can be freely extracted and intercalated back without any alteration. The above measurements indicate that the as-obtained sample exhibits a potential slightly higher than 2 V and a capacity of 278 mA h g^{-1}. All these features are as same as those of bulk β-FeOOH.[7] Since 1D systems, as the smallest dimension structures for efficient transport of electrons, can be applied to detect the theoretical operating limits of lithium batteries,[1] and more and more efforts have been applied to fabricate the nanowire alignment of electrode materials,[6] this route to fabricate nanowire alignment of electrode materials is significant. Certainly further work is desired to reveal how the nanowire alignment of this electrode material improves the performances of lithium batteries.

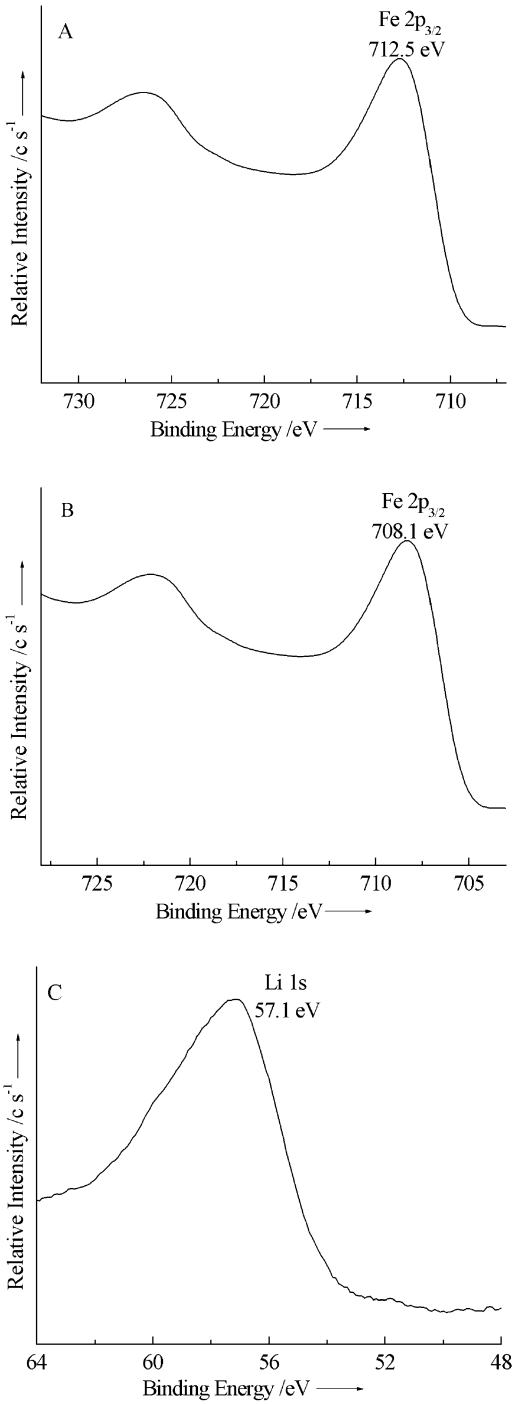

Figure 5. A) Fe 2p core level spectrum of the sample before discharge. B) Fe 2p core level spectrum of the sample after discharge. C) Li 1s core level spectrum of the sample after discharge.

The optical properties of as-obtained product: The optical absorption property of well-aligned β-FeOOH nanowires was investigated with room-temperature (RT) by UV-visible spectroscopy (Figure 6A). Since the onset of the absorption spectrum generally represents the larger end of the size distribution,[16] the position of the absorption onset shows the length of the nanowires. The larger differences between the peak (490 nm) and the onset, which might be related to the width of particle size distribution,[16] are characteristic for nanowires. The spectrum obtained by using the energy as abscissa (Figure 6B) shows that the bandgap of the sample is 2.35 eV. Compared to the reported bandgap of bulk β-FeOOH at 2.12 eV,[8] the substantial blue shift indicates that the β-FeOOH nanowires are quantum confined and have the properties of semiconductor.

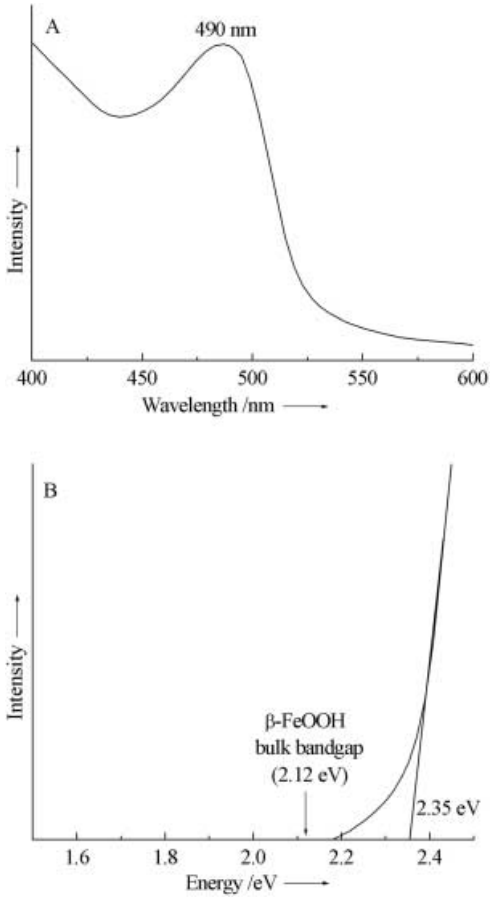

Figure 6. A) UV spectrum of the oriented alignment of β-FeOOH nanowires. B) Spectrum obtained by using the energy as abscissa.

Conclusion

In summary, self-supported patterns of oriented alignment of β-FeOOH nanowires are fabricated by a simple solution reaction from the complex $[Fe(phen)_3]^{2+}$ at 60 °C. The alignment of nanowires with a diameter of 40 nm and length of 6 μm is relatively uniform. HRTEM studies show that the growth direction of β-FeOOH nanowires is vertical to the orientation plane of self-formed β-FeOOH flake-like substrates. The precursor $[Fe(phen)_3]^{2+}$ is undoubtedly vital to the formation of nanowire alignment. In the reaction and crystal growth process, it is thought that the formation of self-supported nanowire alignment results from two competing processes. The characterization of the electrochemical performance and the UV-visible spectrum show that the product is expected to have potential applications in lithium batteries and in the semiconductor industry. This process is simple, mild, clean, reproducible, and free of any template; it provides a new pathway for the low-temperature growth of nanowires and their simultaneous oriented alignment.

Experimental Section

In a typical experiment, $FeCl_2$ (0.50 g, 2.5 mmol) and 1,10-phenanthroline (1.35 g, 7.5 mmol) were loaded into a 125 mL jar that was then filled with H_2O up to 40% of the total volume. Subsequently, the jar was heated at about 4 °C s^{-1} from 25 to 60 °C, and kept at 60 °C for 6 h. All the steps above were carried out with magnetic stirring. The jar was then cooled to room temperature naturally. The precipitate was filtered off, washed with distilled water and absolute ethanol for several times, and then dried in vacuum at 60 °C for 4 h.

For details on the material characterization please see the Supporting Information.

Acknowledgement

This work was supported by the National Natural Science Foundation of China, Chinese Ministry of Education, and Chinese Academy of Sciences. The authors thank Prof. Shuyuan Zhang and Mr. Ke Jiang for technical assistance in HRTEM and FE-SEM experiments, respectively.

[1] a) J. T. Hu, T. W. Odom, C. M. Lieber, *Acc. Chem. Res.* **1999**, *32*, 435; b) M. H. Huang, S. Mao, H. Feick, H. Q. Yan, Y. Y. Wu, H. Kind, E. Weber, R. Russo, P. D. Yang, *Science* **200**1, 292, 1897.
[2] a) H. Masuda, T. Yanagishita, K. Yasui, K. Nishio, I. Yagi, T. N. Rao, A. Fujishima, *Adv. Mater.* **2001**, *13*, 247; b) H. Cao, Z. Xu, H. Sang, D. Sheng, C. Tie, *Adv. Mater.* **2001**, *13*, 121.
[3] M. H. Huang, S. Mao, H. Feick, H. Yan, Y.Wu, H. Kind, E.Weber, R. Russo, P. Yang, *Science* **2001**, *292*, 1897.
[4] a) L. Vayssieres, N. Beermann, S. E. Lindquist, A. Hagfeldt, *Chem. Mater.* **2001**, *13*, 233; b) L. Vayssieres, L. Rabenberg, A. Manthiram, *Nano Lett.* **2002**, *2*, 1393.
[5] Q. Lu, F. Gao, D. Zhao, *Angew. Chem.* **2002**, *114*, 2012; *Angew. Chem. Int. Ed.* **2002**, *41*, 1932.
[6] a) Y. K. Zhou, J. Huang, H. L. Li, *Appl. Phys. A* **2003**, *76*, 53; b) Y. K. Zhou, J. Huang, H. L. Li, *Appl. Phys. B* **2003**, *76*, 53; c) Y. K. Zhou, H. L. Li, *J. Mater. Sci.* **2002**, *37*, 5261.
[7] K. Amine, H. Yasuda, M. Yamachi, *J. Power Sources* **1999**, *81*, 221.
[8] A. F. White, *Rev. Mineral.* **1990**, *23*, 467.
[9] R. M. Cornell, *The Iron Oxides*, VCH, New York, **1996**.
[10] J. W. E. Ceus, J. M. Tacobus, *Chem. Abstr.* **1973**, *78*, 32167m.
[11] Z. W. Pan, Z. R. Dai, Z. L. Wang, *Science* **2001**, *291*, 1947.
[12] a) K. E. Gonsalves, H. Li, P. Santiago, *J. Mater. Sci.* **2001**, *36*, 2461; b) C. X. Gao, Q. F. Liu, D. S. Xue, *J. Mater. Sci. Lett.* **2002**, *21*, 1781; c) K. J. Gallagher, *Nature* **1970**, *226*, 1225; d) J. H. L. Watson, R. R. Cardell, W. Heller, *J. Phys. Chem.* **1962**, *66*, 1757.
[13] F. A. Cotton, G. Wilkinson, *Advanced Inorganic Chemistry*, Wiley, New York, **1972**.
[14] a) E. König, *Coordin. Chem. Rev.* **1968**, *3*, 471; b) K. Madeja, E. König, *J. Inorg. Nucl. Chem.* **1963**, *25*, 377.
[15] C. D. Wanger, W. M. Riggs, L. E. Davis, J. F. Moulder, G. E. Muilenberg, *Handbook of X-Ray Photoelectron Spectroscopy*, Perkin – Elmer, Eden Prairie, **1978**.
[16] T. Tridade, P. O'Brien, X. Zhang, *Chem. Mater.* **1997**, *9*, 523.

Received: May 8, 2003 [F5118]